

# Coupled hydraulic and mechanical model of surface uplift due to mine water rebound: implications for mine water heating and cooling schemes



Fiona Todd<sup>1\*</sup>, Christopher McDermott<sup>1</sup>, Andrew Fraser Harris<sup>1</sup>, Alexander Bond<sup>2</sup> & Stuart Gilfillan<sup>1</sup>

<sup>1</sup> School of Geosciences, University of Edinburgh, Edinburgh, EH9 3FE UK

<sup>2</sup> Quintessa Ltd, Warrington and Henley-on-Thames, UK

FT, 0000-0001-7944-1594; AFH, 0000-0002-8917-8117; SG, 0000-0003-1929-2843

\* Correspondence: [fiona.todd@ed.ac.uk](mailto:fiona.todd@ed.ac.uk)

**Abstract:** In order to establish sustainable heat loading (heat removal and storage) in abandoned flooded mine workings it is important to understand the geomechanical impact of the cyclical heat loading caused by fluid injection and extraction. This is particularly important where significantly more thermal loading is planned than naturally occurs. A simple calculation shows that the sustainable geothermal heat flux from abandoned coal mines can provide less than a tenth of Scotland's annual domestic heating demand. Any heat removal greater than the natural heat flux will lead to heat mining unless heat storage options are also considered.

As a first step, a steady-state, fully saturated, 2D coupled hydromechanical model of a generalized section of pillar-and-stall workings has been created. Mine water rebound was modelled by increasing the hydrostatic pressure sequentially, in line with monitored mine water-level data from Midlothian, Scotland. The modelled uplift to water-level rise ratio of  $1.4 \text{ mm m}^{-1}$  is of the same order of magnitude ( $1 \text{ mm m}^{-1}$ ) as that observed through interferometric synthetic aperture radar (InSAR) data in the coalfield due to mine water rebound. The modelled magnitude of shear stress at the pillar corners, as a result of horizontal and vertical displacement, is shown to increase linearly with water level. Mine heat systems are expected to cause smaller changes in pressure than those modelled but the results provide initial implications on the potential geomechanical impacts of mine water heat schemes which abstract or inject water and heat into pillar-and-stall coal mine workings.

**Thematic collection:** This article is part of the SJG Collection on Early-Career Research available at: <https://www.lyellcollection.org/cc/SJG-early-career-research>

**Received** 14 December 2018; **revised** 26 June 2019; **accepted** 3 July 2019

The utilization of abandoned flooded mine workings in the UK could provide a renewable heat source near to centres of population. Hence, interest in extraction of this resource has recently increased partially driven by analysis which indicates that the UK will fail to meet legally binding renewable energy targets by 2020. There is also increasing awareness that progress in renewable heat is essential to overall decarbonization goals (House of Commons Energy and Climate Committee 2016). Heating accounts for over half of Scotland's energy use and currently renewable sources contribute less than 5% to this (The Scottish Government 2018).

It has been estimated that a third of Scotland's heating requirement could be obtained by utilizing shallow abandoned coal mine workings (Gillespie *et al.* 2013) although this may be considered 'heat mining', i.e. abstracting more than is sustainable. A high level estimate of the geothermal heat flow ( $65 \text{ mW m}^{-2}$ ) and the area mined in the Midland Valley ( $4.8 \times 10^3 \text{ km}^2$  taken from (Gillespie *et al.* 2013)) suggests that the amount of geothermal energy available annually is  $9.8 \times 10^9 \text{ MJ}$ , i.e. around 8% of Scotland's annual domestic heating demand. Any more heat removal will inevitably lead to non-sustainable heat mining unless heat storage options are also considered. The potential for mine

source heat energy globally is significant, with 3000 MW potentially available from flooded mines throughout Europe (Bailey *et al.* 2016) and it is thought that there are more than 1 million abandoned mines throughout the world (Hall *et al.* 2011).

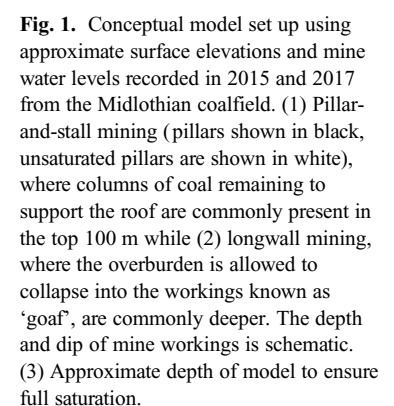
Mine water heat schemes have been operational since the 1980s (Jessop 1995) and the first trials for operational schemes in Scotland were undertaken in the early 1990s (Banks *et al.* 2009). Interest in the renewable heat energy potential of UK mine workings has seen a recent resurgence (e.g. Bailey *et al.* 2016; Farr *et al.* 2016). Feasibility studies of the potential of abandoned coal mine workings have been funded in Scotland (Harnmeijer *et al.* 2012) and Wales (Department for Business Energy & Industrial Strategy 2018) and pilot schemes have been installed at two former collieries in England (Banks *et al.* 2019). One of two new UK Geoenergy Observatories is located in Glasgow to specifically research the mine water environment in the context of developing mine water heat technology (Monaghan *et al.* 2018).

Mine workings that are at shallower depths, closer to the ground surface are typically the oldest workings and many were abandoned with intact coal columns (pillars/stoops) for stability (NCB 1972; Younger & Robins 2002). These pillars

This paper describes a coupled hydraulic and mechanical model of a flooded abandoned pillar-and-stall mine system under increasing hydraulic head. It provides a first stage understanding of the geomechanical response to variations in

- (1) conceptual modelling of the mine water system;
- (2) model parameterization of a generic coal mine workings geometry;
- (3) numerical finite element modelling to determine geomechanical impacts on pillar properties through rising water levels;
- (4) results and limitations of the model.

Fluid and heat flow pathways are dependent on the volume mined and dewatered, which is related to the type of mining (Wolkersdorfer 2008). This research has focused on coal mines worked by hand following the pillar-and-stall (also known as stoop-and-room or bord-and-pillar) method (Fig. 1). This is where props held up the formation while explosives were used, the coal was then hand-stripped out



and stoops or pillars of coal were left to maintain the integrity of the workings. Traditional pillar design is based on the principle that the strength of the pillar must be greater than the load placed upon it (NCB 1975; Jaiswal & Shrivastva 2009).

This method of working continued in the UK up until mechanization was brought in around the 1950/1960s. In longwall mining conveyors were used next to the coalface and the whole area of coal was removed with the ceiling allowed to collapse behind it. Pillar-and-stall mining was still used where the dip of the workings was too great for shearing machine access. These shallower systems provide the most accessible source of heat. As pillar-and-stall workings tend to rely on the pillars for stability, it is likely that any instability induced from a changing water level will be more likely to impact these workings compared to longwall workings which have usually already collapsed and are generally infilled with goaf (i.e. collapsed overburden).

Geological systems are inherently complex and simplification is necessary to represent the controlling mechanisms (Kruse & Younger 2009). Mining systems, in particular, have a number of site-specific characteristics (e.g. seam thickness, number of seams worked, mining arrangement), producing a unique hydraulic system; assumptions have to be made to allow creation of a representative conceptual model. The main hydrogeological components of a mining system are similar to an unworked aquifer: recharge, regional groundwater flow and leakage from and to underlying confined aquifers. Mine-specific elements include water ingress through open workings (e.g. shafts, near-surface workings), leakage from the formation into open mine workings and water inflow from adjacent connected mines. Mines can be considered to have triple porosity: primary porosity of rock, mining voids and additional fractures caused by mining (Andrés *et al.* 2017), which adds complexity to the flow mechanisms. There is the added complication that fluid flow is dependent on the groundwater rebound situation; turbulent flow becomes important when large open voids are refilling (Adams & Younger 2001).

As a simplification, the model that has been developed here assumes that the mine workings are fully saturated (i.e. water in place) and the effects of recharge, leakage (both mining related and not) and ingress from non-flooded workings have not been addressed. The model reflects rising groundwater, i.e. mine water rebound, which has been modelled through pressure changes over a number of steps with time. It is assumed that there is no regional groundwater gradient.

Surface uplift due to mine water-level rebound has been identified in several coal mining areas, e.g. South Wales (Bateson *et al.* 2015) and Northumberland (Gee *et al.* 2017) but not modelled through a hydromechanical model. The rising water level increases pore pressure in the overburden and in mining-related disturbed zones, causing expansion which can result in surface uplift. This uplift is considered to have a linear relationship with mine water level (Bekendam & Pottgens 1995) as deformation is calculated as a function of effective stress (equations 3–5). There could also be some minor elastic rebound and local scale uplift due to the reduction in vertical effective stress by the rising water level (Bateson *et al.* 2015).

This research has excluded any mining-induced fractures and has assumed that the mine workings are intact and the stalls are essentially fully saturated voids. In reality, in some places the workings will have collapsed leaving waste material ‘goaf’ in the stalls which will provide some mechanical stability to the system. Flow is governed by Darcy’s Law and the stall material has been given properties representative of water, i.e. flow will preferentially occur in the stalls compared to the surrounding material and is flowing from the base of the model to the top to simulate rebounding groundwater levels.

The materials included in the model are assumed to be homogeneous and isotropic, which is a significant simplification, as the strata surrounding the flooded mine workings are generally highly stratified with different geomechanical responses. Storage has not been included at this stage, i.e. calculations were performed assuming a steady state. Deformation associated with groundwater-level rise is assumed to be an elastic process and, as such, a linear elastic constitutive model has been applied at this stage; plastic deformation has not been considered.

### *Model parameterization*

#### *Geometry*

The model developed in this research is a generic pillar-and-stall system; however, several attributes are based on mine workings in part of the Midlothian coalfield. This area has been selected as it is known there are pillar-and-stall workings present and, more significantly, surface uplift has been recorded in recent data (2015–17) which has been attributed to rising mine water (GVL 2018), providing data to test the model.

The Midlothian area is between Penicuik and Dalkeith, approximately following a north–east-trending syncline. The mining history is complex, with recorded mining from the seventeenth century which became progressively deeper as the shallow coal was exhausted. There were more than ten operational collieries before post-nationalization closures began in the 1950s. Lady Victoria and Bilston Glen were the last to cease production in the late 1980s (Northern Mine Research Society, <https://www.nmrs.org.uk/>). Mine water levels were controlled during operations by a complex network of pumping shafts; latterly pumps in Bilston Glen and Easthouses shafts managed the water in the west and east of the area respectively. Bilston Glen dewatered the whole area following closure of Easthouses in 1969 (URS 2014). It is assumed mine water pumping stopped around the same time as Bilston Glen closed, in 1989.

Mine water level is recorded monthly from shafts at Bilston Glen and Easthouses by the Coal Authority. The rate of rebound at Bilston Glen has reduced over time, from around 21 m a<sup>-1</sup> between 2006 and 2010 (URS 2014) to around 18 m a<sup>-1</sup> between 2010 and 2014 (data supplied by The Coal Authority). Between 2015 and 2017 the water levels rose from –10 mAOD to 27 mAOD (metres above ordnance datum), equivalent to 164 m and 127 m below surface, respectively, a rate of nearly 13 m a<sup>-1</sup> (Fig. 2). Data from 2013 for Easthouses, which is c. 7 km east of Bilston Glen, show the water level in this part of the mine system follows the same pattern of rebound, indicating the mine

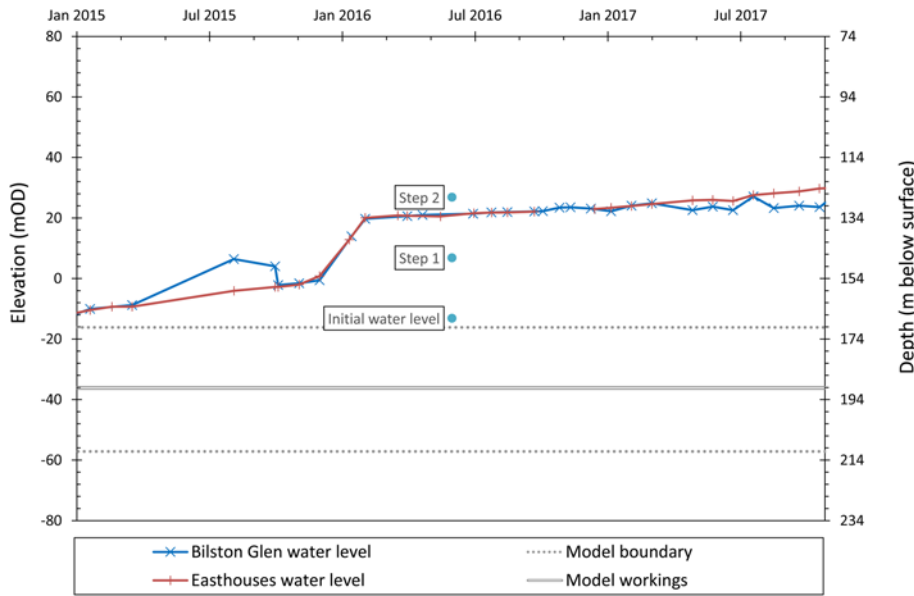


**Fig. 2.** Recorded mine water level at Bilston Glen and Easthouses colliery shafts between 2015 and 2017 (both in metres relative to ordnance datum (OD) and below surface). The depth of the modelled mine workings (based on Bilston Glen ground level) is shown at the bottom of the diagram to illustrate the position relative to the measured water level (i.e. the modelled hydraulic head). The water levels used in each model step are also shown. Mine water data reproduced with the permission of © The Coal Authority.

workings are connected. The large increase in water levels in the 2015/2016 winter seen in Figure 2 is thought to be the result of additional water make/inflow from a previously unconnected section of workings.

As a simplification the model has been assumed to be fully saturated, meaning the top of the workings must be below the deepest water level, shown by a dotted line on Figure 1. The depth of the modelled mine workings relative to measured water levels is shown on Figure 2. In order to use the measured water-level data, the modelled workings were set at 190 m with 20 m of overburden and underburden; this is considered to be sufficient to avoid boundary condition influences. The modelled conditions are therefore potentially deeper than typical pillar-and-stall workings.

The additional unmodelled overburden was included as a source term (mechanical boundary load), representing lithostatic pressure using the following equation:

$$P_{ST} = \rho_{\text{overburden}} g h \quad (1)$$

where  $P_{ST}$  is the calculated source term pressure (Pa),  $\rho_{\text{overburden}}$  is the estimated mean density of the overburden ( $\text{kg m}^{-3}$ ),  $g$  is gravitational acceleration ( $\text{m s}^{-2}$ ) and  $h$  is the thickness of overburden from the top of the model to the surface (m).

The dimensions of pillars in this location are highly irregular and are dependent on the specific conditions encountered during mining. Abandoned coal mine plans indicate that the pillar sizes can range from around  $5 \times 5$  m to  $>30 \times 15$  m. A pillar width of 12 m was chosen for the model, representing an average of those measured.

The stall width is dependent upon the volume of material mined and also on the strength of the local overburden lithology. The range of estimates for pillar-and-stall extraction is large, between 15–90% (Gee *et al.* 2017) and 30–60% (Edmonds 2018) material removed. A low extraction of *c.* 30% was used in this model to give a stall width of 6 m. These dimensions are within typical dimensions for Carboniferous Coal Measures: stalls were generally 6 to 9 m wide and pillars 9 to 30 m wide (Younger & Adams 1999). The model is a conservative scenario with respect to pillar

failure; if the stalls were larger, i.e. a higher extraction, then the pressure on the pillars would be larger due to the greater span between them. The height of the pillar is dependent on the particular coal seam thickness; an average value of 1 m was taken from graphs comparing pillar width, overburden cover depth and road height (NCB 1972). The model comprises one level of flooded workings with five pillars (Fig. 3).

#### Boundary conditions

The deformation boundary conditions are shown in Figure 3, with the bottom boundary completely static and the other boundaries allowed to move vertically but not horizontally. Fluid pressure boundary conditions were set at the top and bottom of the model to represent hydrostatic pressure. Initially the hydrostatic pressure was based on a water level of 167 m below the surface, taken from Figure 2. Two additional steps were run, each corresponding to 20 m water-level rise, with the final water level at 127 m below surface. This is equivalent to the overall rise experienced at

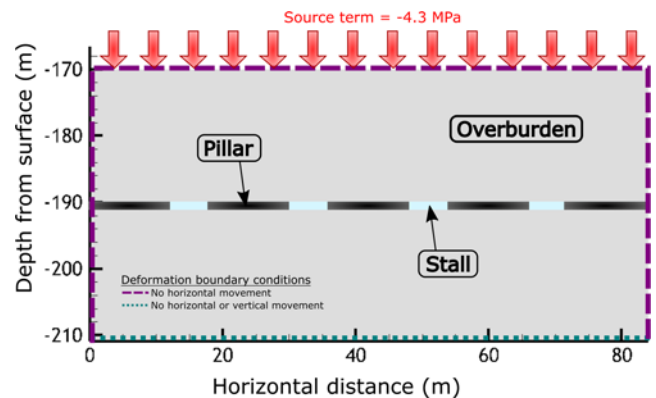


**Fig. 3.** Schematic showing numerical model set-up. Three material groups were modelled as shown: overburden/underburden, pillar (coal) and stall (water). The deformation boundary conditions at the model edges are as shown, with only the model base fully static. A lithostatic pressure source term is added from the top to represent the unmodelled overburden from surface to model top. Fluid pressure boundary conditions are also added to the top and bottom of the model to represent hydrostatic pressure.

Bilston Glen from 2015 to 2017; the actual rate of rise has been averaged to simplify the modelling process.

### Material properties

The geology of this area comprises layered sedimentary rocks of both the Clackmannan Group and the Scottish Coal Measures Group which were deposited during the Carboniferous Period. Bilston Glen is located on the western edge of a syncline, with collieries such as Easthouses, Lingerwood and Lady Victoria positioned on the eastern side. The shallowest layers of this syncline are from the Coal Measures Group, with deeper sandstones and cyclical coal- and limestone-bearing sequences of the Clackmannan Group. The overburden and underburden are assumed to be homogeneous and have been given material properties related to the Coal Measures (Table 1; Malolepszy 2003; BGS 2015). The material properties for the coal pillars are taken from generic values for coal, again assumed to be homogeneous (Durucan & Edwards 1986; Holloway *et al.* 2002; Malolepszy 2003; Ordóñez *et al.* 2012).

Deformation of saturated rock is controlled by the material-dependent properties of rock stiffness, confining stress and pore pressure (Ma & Zoback 2017), i.e. the effective stress. The elastic parameters of Young's modulus and Poisson's ratio (the ratio of lateral to longitudinal strain) are required for the model calculations. A full sensitivity analysis of these parameters has not been undertaken at this stage; standard literature values for sedimentary sandstones/limestones (Duncan Fama *et al.* 1995; Dethlefsen *et al.* 2016) and coal (Murali Mohan *et al.* 2001; Salmi *et al.* 2017) were given to the overburden and pillars respectively, as summarized in Table 1.

The material properties of the water-filled stalls are more complex to determine, as water does not behave as a rock material. The stalls were assumed to be fully porous (i.e. 100%) and the density of water ( $1000 \text{ kg m}^{-3}$ ) was used. Model analysis was undertaken on the impact of varying the permeability of the stalls and a value of  $10^{-10} \text{ m}^2$  was considered appropriate for this continuum model. A Young's modulus value two orders of magnitude smaller was considered small enough to allow differentiation with the rock while not causing modelling instability. The Poisson's ratio of 0.25 was given, making it consistent with the other materials.

### Numerical modelling approach

Research into modelling mine water heat schemes has focused on heat extraction and flow transfer in mines ranging from analytical solutions to 3D numerical models. The inclusion of geomechanical processes in this research has meant a numerical solution is more appropriate than an

analytical solution. Several different numerical codes covering finite difference, finite element and finite volume solutions have been used to model heat and flow transport processes in mines; a full review can be found in Loredó *et al.* (2016). None of these models has included geomechanical processes and few of the modelling codes used previously have the capability of solving the geomechanical governing equations alongside heat and fluid flow processes. The modelling code used in this study is OpenGeoSys (<https://www.opengeosys.org/>) (Kolditz *et al.* 2012); a finite element open source code specifically developed for coupled thermo-hydro-geomechanical–chemical (THMC) processes in porous and fractured media. This established code is used to simulate uplift in a complex system as a precursor to understanding stresses in the overburden and underburden at the pillars due to the superposition of the mechanical, thermal and hydraulic signals.

To ensure simplicity of calculations the model was constructed as a fully saturated, steady-state system in 2D. The mesh was created using Gmsh (Geuzaine & Remacle 2009), with triangular elements, node spacing ranged from 0.5 m at the workings to 1.4 m at the model extremities.

Simulations for this research were performed through coupled hydraulic–mechanical processes. Hydraulic flow is calculated using Darcy's law for a saturated media (Freeze & Cherry 1979):

$$Q = \nabla \left( \frac{k}{\mu} (\nabla p + \rho_{\text{fluid}} g \nabla z) \right) \quad (2)$$

where  $Q$  is the volumetric flow rate ( $\text{m}^3 \text{ s}^{-1}$ ),  $p$  is pressure (Pa),  $t$  is time (s),  $k$  is intrinsic permeability of the rock ( $\text{m}^2$ ),  $\mu$  is dynamic viscosity of the fluid ( $\text{kg m}^{-1} \text{ s}^{-1}$ ),  $\rho_{\text{fluid}}$  is fluid density ( $\text{kg m}^{-3}$ ),  $g$  is gravitational acceleration ( $\text{m s}^{-2}$ ) and  $z$  is the depth to the datum (m). The modelling was calculated using steady-state conditions. Deformation of a body is calculated by the momentum balance equation, in terms of stress as (Wang *et al.* 2009):

$$\nabla \sigma + \rho g = 0 \quad (3)$$

where  $\sigma$  is the stress tensor. Stress is related to strain via a constitutive relationship. In this case Hooke's Law of linear elasticity has been used, whereby the resulting strain is proportional to the applied stress:

$$\sigma = E e \quad (4)$$

where  $E$  is Young's modulus and  $e$  is the strain. The model makes the assumption of plane strain in 2D and is solved using a linear iterative method. Modelling the deformation of saturated mine workings requires coupling of the hydraulic process with the mechanical process via poro-elasticity. This

**Table 1.** Material properties used in model

Material type	Porosity $\eta$	Permeability $k \text{ (m}^2\text{)}$	Density $\rho \text{ (kg m}^{-3}\text{)}$	Young's modulus $E \text{ (Pa)}$	Poisson's ratio $\nu$
Overburden	0.15 [1]	$1.2 \times 10^{-13}$ [1]	2600 [2]	$2.5 \times 10^8$ [3]	0.25 [4, 5]
Pillar (coal)	0.02 [6]	$1.0 \times 10^{-14}$ [7]	1500 [8]	$4.0 \times 10^8$ [9]	0.25 [4]
Stall (water)	1.00	$1.0 \times 10^{-10}$	1000	$2.5 \times 10^6$	0.25

Sources in square brackets: <sup>1</sup>BGS (2015), <sup>2</sup>Malolepszy (2003), <sup>3</sup>Dethlefsen *et al.* (2016), <sup>4</sup>Murali Mohan *et al.* (2001), <sup>5</sup>Duncan Fama *et al.* (1995), <sup>6</sup>Holloway *et al.* (2002), <sup>7</sup>Durucan & Edwards (1986), <sup>8</sup>Ordóñez *et al.* (2012), <sup>9</sup>Salmi *et al.* (2017).

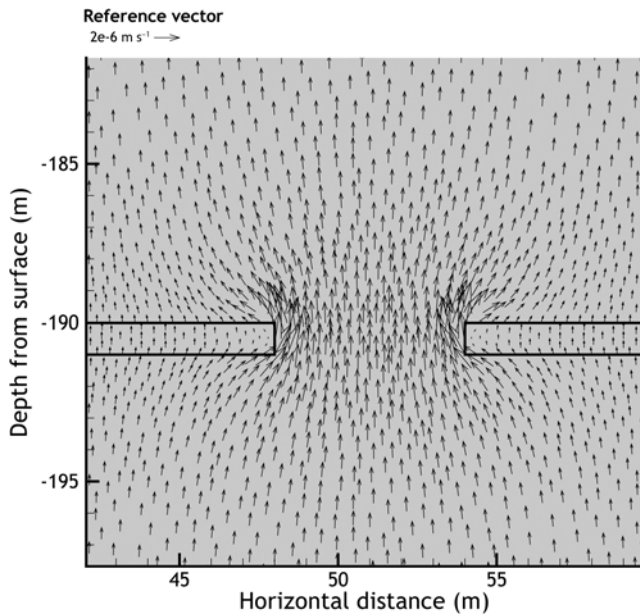


Fig. 4. Fluid velocity vectors output from the model, focusing on the velocity vectors around two pillars in cross section.

is achieved through the concept of effective stress for porous media, which states that the actual stress resulting in a deformation is a function of the fluid pressure and the stress conditions. This is determined from:

$$\sigma' = \sigma - \alpha P \quad (5)$$

where  $\sigma'$  is the effective stress (Pa),  $\sigma$  is the stress (Pa),  $P$  is the fluid pressure (Pa), and  $\alpha$  is the Biot coefficient (–). The Biot coefficient is a poro-elastic coupling parameter that is essentially the ratio of fluid pressure to transferred rock pressure (McDermott *et al.* 2016). A value of 1 was used in this model as a representative estimate, whereby all changes in the fluid pressure are transferred to the rock which is realistic for this model set-up.

## Discussion

### Results

The fluid velocity results output from the model are presented as vectors in Figure 4, showing two pillars

(outlined in black) with the stall in between. These vectors show that fluid will preferentially flow through the stalls, which is as expected, as this is the most permeable layer. The overall direction of flow is from the base of the model to the top, which is as expected when no regional groundwater gradient is considered. These results provide reassurance that the model can be used to assess the impacts of rising groundwater levels on the mine workings.

Surface uplift in the area of interest has been measured as around  $8 \text{ mm a}^{-1}$  between October 2015 and 2017 (GVL 2018) and this has been attributed to mine water rebound (Sowter *et al.* 2017). This uplift was measured by processing Sentinel-1 satellite data using InSAR software to produce average velocity maps (GVL 2018).

A total water-level rise of 40 m (167–127 m below surface) was modelled in two 20 m steps, representing the field data presented in Figure 2. The differential results have been assessed as compared to the initial water level. The modelled vertical displacement (Fig. 5) shows that rising water level leads to uplift of the whole rock volume. An uplift of 55 mm for a water-level rise of 40 m was calculated at the top of the model. This equates to 1.4 mm uplift for every 1 m of water-level rise compared to the measured uplift of *c.* 1 mm uplift per 1 m of water-level rise (based on GVL and Coal Authority data).

The differences between 20 m and 40 m water-level rise are clear; the displacement for a water-level increase of 40 m is double that for a water-level rise of 20 m: 55 mm compared to 27.5 mm. This proportionality is as expected given the uniform material properties and steady-state nature of the model.

A detailed view of the displacement around the edges of the pillars is shown in Figure 6, again for both the 20 m and 40 m rise in water level. The mesh of the model is shown in grey. The material in between each pillar (pillars outlined in black) is the water-filled stall which, due to the mechanical properties, shows a higher displacement than around the pillars.

The horizontal and vertical displacement around the pillar edges is of interest as this is where stress is likely to build up and cause weakening of the pillar over time. Figure 7 shows the differential displacement in the horizontal direction

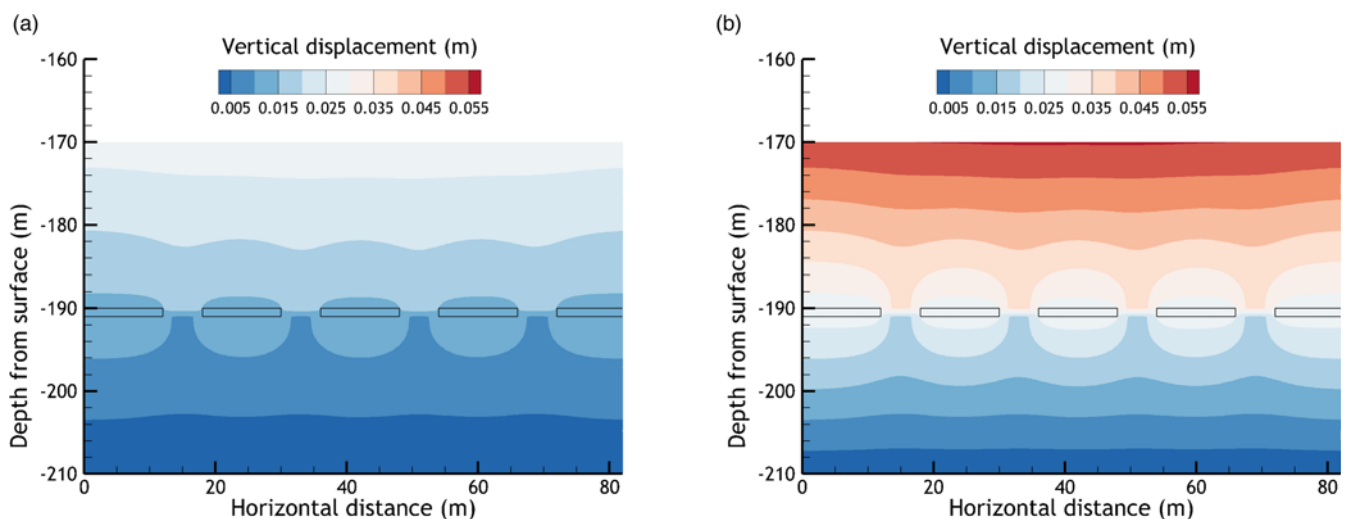
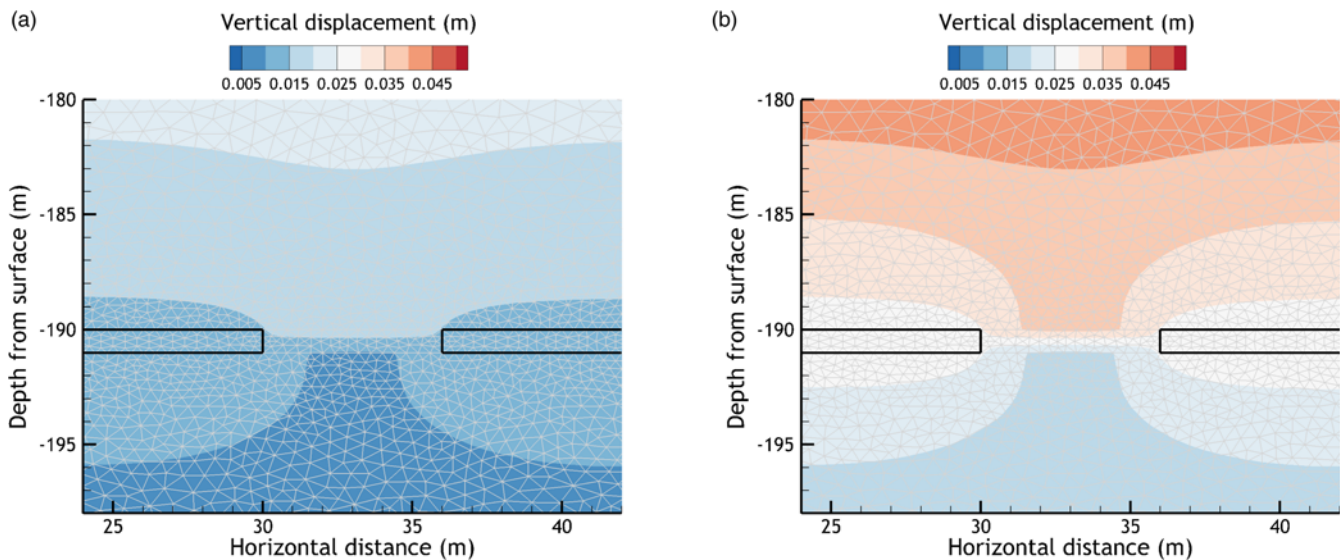


Fig. 5. Cross-section of full model showing modelled differential vertical displacement for a head change of (a) 20 m and (b) 40 m.



**Fig. 6.** Cross-section for one stall and two pillars (outlined in black) showing detail of modelled differential vertical displacement around pillar for a head change of (a) 20 m and (b) 40 m.

where the lateral movement of the pillar into the stall space can be seen. This occurs due to the difference in Young's modulus between the two materials. The horizontal displacement increases with increasing pressure (water level). The maximum horizontal displacement is an order of magnitude lower than the maximum vertical displacement: 0.002 m compared to 0.055 m.

The component of shear stress is important in determining pillar stability; the modelled results are shown in Figure 8. Due to the displacements shown in Figures 6 and 7, the shear stress is highest at the corners of the pillars and the magnitude is approximately doubled from 0.15 MPa to 0.30 MPa with a doubling in head.

These results highlight the impact of water-level changes on the stresses placed on flooded pillar-and-stall workings, specifically the interaction between the pillar edge and the water-filled void next to it. The differential horizontal displacement is largest at the edges of the pillars,

emphasizing the changes the pillar undergoes with a rising water level. The shear stress seen at the edges of the pillars is also significant as this is the likely location where stress could build up. The modelled stresses are low compared to rock-strength values but future work is needed to test if small changes to critically stressed zones could lead to rock failure.

#### Model limitations

This model simulates the geomechanical impact on a single layer of saturated pillar-and-stall workings as a result of rising water level. As this is a generic steady-state model it does not take into account site-specific factors such as the dip of mine workings and strata, or mechanical and storage properties of the overburden between the top of the model and ground level.

Initial analysis indicates that the depth of workings, modelled through changing the geometry and the lithostatic

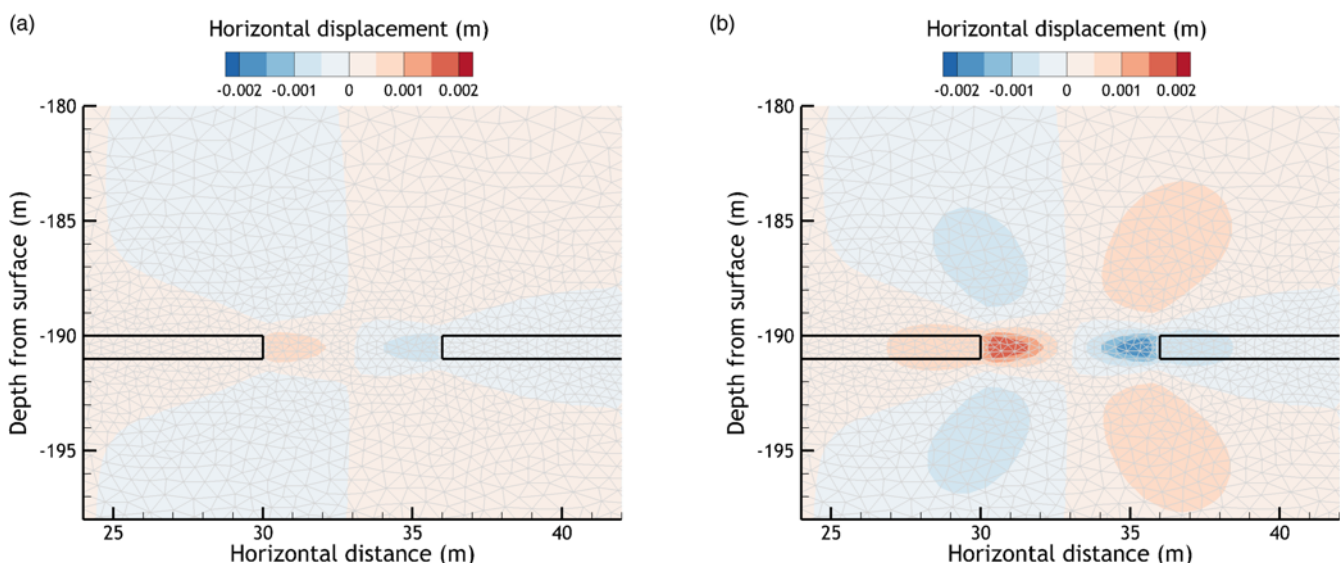


**Fig. 7.** Cross-section for one stall and two pillars (outlined in black) showing modelled differential horizontal displacement around pillars for a head change of (a) 20 m and (b) 40 m.

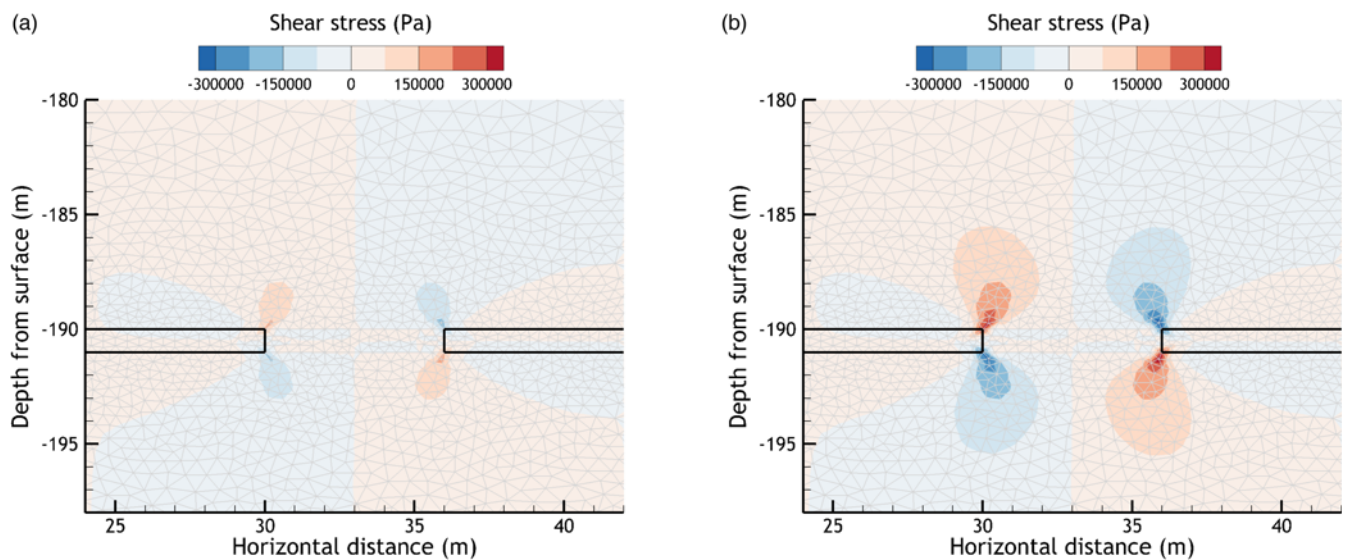


Fig. 8. Cross-section for one stall and two pillars (outlined in black) showing modelled differential shear stress for a head change of (a) 20 m and (b) 40 m.

pressure source term, has no impact on the magnitude and direction of the resultant modelled displacements and stresses (Fig. 9). This is due to the model set-up and overburden being assumed to be homogeneous and isotropic.

In reality, there will also be regional groundwater flow which could impact the hydraulic pressure values and subsequently the deformation results and, as indicated above, modelling the water-filled stalls with equivalent mechanical material properties is complex. Nevertheless, the modelled uplift to water-level rise ratio is of the same order of

magnitude to that observed ( $1.4 \text{ mm m}^{-1}$  and  $1 \text{ mm m}^{-1}$  respectively, providing confidence in the methodology and a strong basis from which to develop a site-specific model.

#### Future work

This model highlights the results for a simple case of rising mine water level, it is the first step in understanding the geomechanical response of flooded pillar-and-stall workings to changes in hydrostatic pressure. The next stages of

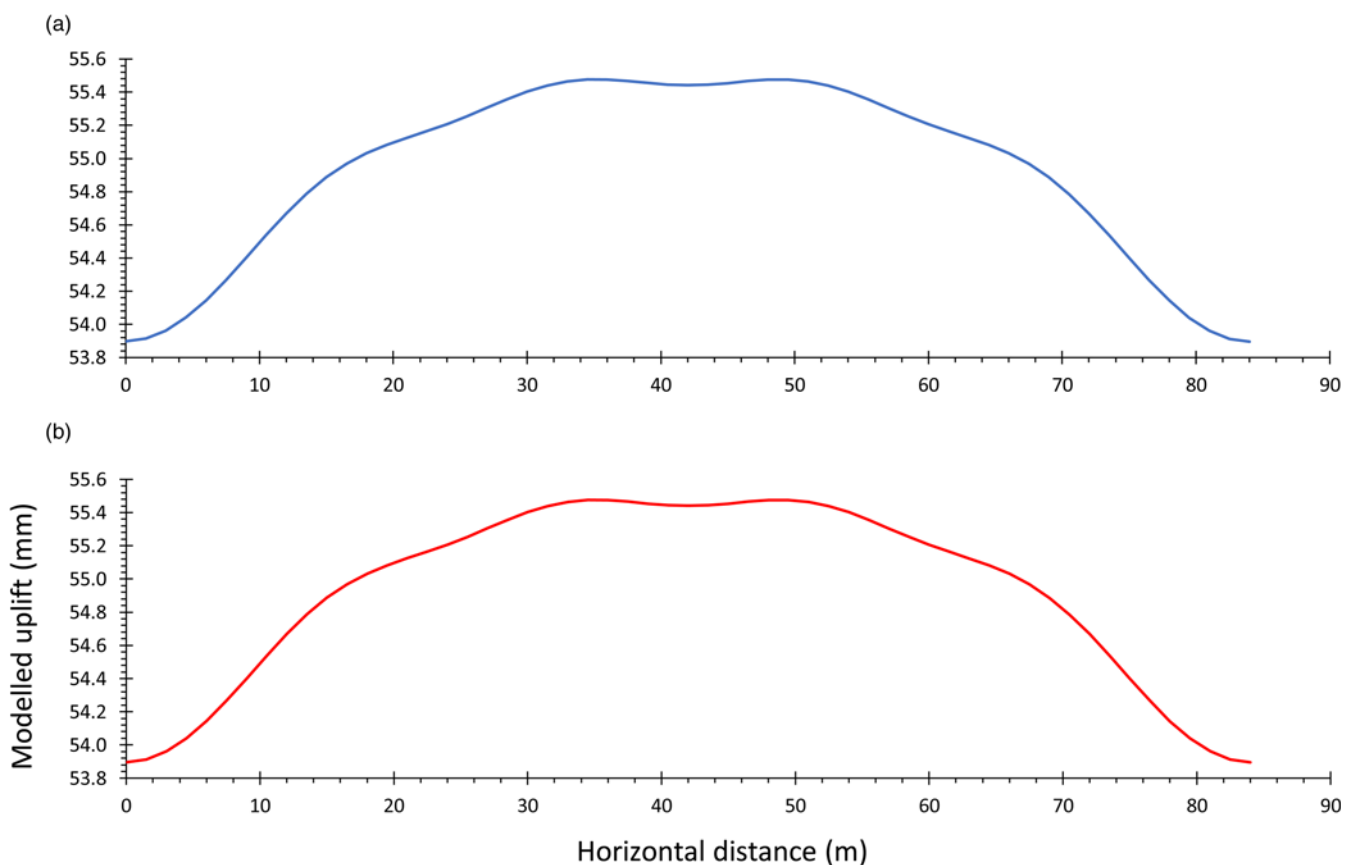


Fig. 9. Graphs showing modelled vertical displacement (uplift) along top boundary of models with one layer of mine workings at (a) 190 m depth and (b) 250 m depth.

modelling will aim to understand how displacements and stresses are dissipated through a layered heterogeneous overburden and underburden, which will also include multiple layers of workings that are likely to influence the deformation profile. The impact of changing saturation (i.e. water level) on the overburden properties will also be investigated.

The main aim of future work will be to develop the model to understand the impacts of mine water heating/cooling schemes on the integrity of pillar-and-stall workings. Mine water heat systems are likely to abstract and inject water cyclically, depending on heating and cooling needs and storage requirements. These systems are expected to cause smaller changes in water level and pressure than those modelled but any critically stressed rock could fail due to small changes in stress conditions. It is also known that rock fatigue is important in cyclical systems. Even small changes in stress amplitudes can cause fatigue, resulting in rock failure (Preisig *et al.* 2016). An important next step will be to determine failure criteria for the pillars, based on rock-strength properties. The model will also be developed to include the coupling of heat transport and transient conditions.

## Conclusions

This paper describes a method to assess the impacts of rising water on saturated pillar-and-stall workings. It has focused on the development of a preliminary, generic coupled hydraulic and geomechanical model with one layer of workings, including five pillars and four stalls. Rising mine water levels were modelled through increasing hydrostatic pressure above the workings.

Increasing fluid pressure results in a modelled uplift of 55 mm caused by a decrease in effective stress. This deformation, combined with the geometry of the pillars and stalls, leads to minor stress concentrations at the edges of the water-filled stalls. The magnitude of this is modelled to increase linearly with increasing water level/fluid pressure.

Rising mine water levels resulted in a modelled uplift to water-level rise ratio of  $1.4 \text{ mm m}^{-1}$ , which is in the same order of magnitude to that observed in Midlothian, Scotland of  $1 \text{ mm m}^{-1}$  due to mine water rebound. The results provide a valuable understanding of the potential geomechanical impacts of mine water heat schemes which abstract or inject water and heat into pillar-and-stall coal mine workings.

The simulated uplift is a precursor to understanding the stress in the overburden and underburden at the pillars due to the superposition of the mechanical, thermal and hydraulic signals associated with mine water heat schemes. This model validates the hydraulic and mechanical coupling at a regional scale. Planned future work will develop the model further with the aim of understanding the impacts of mine water heating/cooling and storage schemes on the integrity of pillar-and-stall workings.

**Acknowledgements** The authors would like to thank Lee Wyatt at the Coal Authority for information regarding the Midlothian coalfield. We thank two reviewers for their constructive comments which have greatly improved the manuscript.

**Funding** This work was supported by a NERC Doctoral Training Partnership grant (NE/L002558/1) and funded by Quintessa Ltd through a CASE sponsorship.

**Author contributions** FT: Formal analysis (Lead), Methodology (Lead), Visualization (Lead), Writing – Original Draft (Lead); CM: Conceptualization (Lead), Formal analysis (Supporting), Software (Lead), Supervision (Lead), Writing – Review & Editing (Equal); AFH: Formal analysis (Supporting), Methodology (Supporting), Supervision (Supporting), Visualization (Supporting), Writing – Review & Editing (Equal); AB: Conceptualization (Supporting), Supervision (Supporting), Writing – Review & Editing (Equal); SG: Supervision (Supporting), Writing – Review & Editing (Supporting)

*Scientific editing by Heather Stewart*

## References

- Adams, R. & Younger, P.L. 2001. A strategy for modeling ground water rebound in abandoned deep mine systems. *Groundwater*, **39**, 249–261, <https://doi.org/10.1111/j.1745-6584.2001.tb02306.x>
- Andrés, C., Ordóñez, A. & Álvarez, R. 2017. Hydraulic and thermal modelling of an underground mining reservoir. *Mine Water and the Environment*, **36**, 24–33, <https://doi.org/10.1007/s10230-015-0365-1>
- Bailey, M.T., Gandy, C.J., Watson, I.A., Wyatt, L. & Jarvis, A.P. 2016. Heat recovery potential of mine water treatment systems in Great Britain. *International Journal of Coal Geology*, **164**, 77–84, <https://doi.org/10.1016/j.coal.2016.03.007>
- Banks, D., Fraga Pumar, A. & Watson, I.A. 2009. The operational performance of Scottish minewater-based ground source heat pump systems. *Quarterly Journal of Engineering Geology and Hydrogeology*, **42**, 347–357, <https://doi.org/10.1144/1470-9236/08-081>
- Banks, D., Athresh, A., Al-Habaibeh, A. & Burnside, N.M. 2019. Water from abandoned mines as a heat source: practical experiences of open- and closed-loop strategies, United Kingdom. *Sustainable Water Resources Management*, **5**, 29–50, <https://doi.org/10.1007/s40899-017-0094-7>
- Bateson, L., Cigna, F., Boon, D. & Sowter, A. 2015. The application of the intermittent SBAS (ISBAS) InSAR method to the South Wales Coalfield, UK. *International Journal of Applied Earth Observation and Geoinformation*, **34**, 249–257, <https://doi.org/10.1016/j.jag.2014.08.018>
- Bekendam, R.F. & Pottgens, J.J. 1995. Ground movements over the coal mines of southern Limburg, The Netherlands, and their relation to rising mine waters. *Proceedings of the Fifth International Symposium on Land Subsidence*, IAHS Publication No 234.
- Beveridge, R., Brown, S., Gallagher, M. & Merrit, J. 1991. Economic geology. In: Craig, G. (ed.) *Geology of Scotland*. Geological Society, London, 545–595.
- BGS 2015. *Scotland's Aquifers and Groundwater Bodies*. Groundwater Science Programmes.
- Department for Business Energy & Industrial Strategy 2018. *SSH Phase 2 D37/ D38: Smart Energy Plan—Bridgend County Borough Council*.
- Detlefsen, F., Beyer, C., Feeser, V. & Köber, R. 2016. Parameterizability of processes in subsurface energy and mass storage: Supported by a review of processes, codes, parameters, and a regional example: Schleswig-Holstein, Germany. *Environmental Earth Sciences*, **75**, 885, <https://doi.org/10.1007/s12665-016-5626-1>
- Diez, R.R. & Diaz, M.B. 2014. Estimating limits for the geothermal energy potential of abandoned underground coal mines: A simple methodology. *Energies*, **7**, 4241–4260, <https://doi.org/10.3390/en7074241>
- Duncan Fama, M.E., Trueman, R. & Craig, M.S. 1995. Two- and three-dimensional elasto-plastic analysis for coal pillar design and its application to highwall mining. *International Journal of Rock Mechanics and Mining Sciences and Geomechanics Abstracts*, **32**, 215–225, [https://doi.org/10.1016/0148-9062\(94\)00045-5](https://doi.org/10.1016/0148-9062(94)00045-5)
- Durucan, S. & Edwards, J.S. 1986. The effects of stress and fracturing on permeability of coal. *Mining Science and Technology*, **3**, 205–216, [https://doi.org/10.1016/S0167-9031\(86\)90357-9](https://doi.org/10.1016/S0167-9031(86)90357-9)
- Edmonds, C. 2018. Five decades of settlement and subsidence. *Quarterly Journal of Engineering Geology and Hydrogeology*, **51**, 403–416, <https://doi.org/10.1144/qjegh2018-089>
- Farr, G., Sadasivam, S., Manju, Watson, I.A., Thomas, H.R. & Tucker, D. 2016. Low enthalpy heat recovery potential from coal mine discharges in the South Wales Coalfield. *International Journal of Coal Geology*, **164**, 92–103, <https://doi.org/10.1016/j.coal.2016.05.008>
- Ferket, H.L.W., Laenen, B.J.M. & Van Tongeren, P.C.H. 2011. Transforming flooded coal mines to large-scale geothermal and heat storage reservoirs: what can we expect? In: Rüde, T.R., Freund, A. & Wolkersdorfer, C. (eds) *International Mine Water Association Congress Proceedings – Mine Water – Managing the Challenges*, 171–176.
- Freeze, R.A. & Cherry, J.A. 1979. *Groundwater*. Englewood Cliffs. Prentice Hall.
- Gee, D., Bateson, L. *et al.* 2017. Ground Motion in Areas of Abandoned Mining: Application of the Intermittent SBAS (ISBAS) to the Northumberland and Durham Coalfield, UK. *Geosciences*, **7**, 85, <https://doi.org/10.3390/geosciences7030085>
- Geuzaine, C. & Remacle, J. 2009. Gmsh: A 3-D finite element mesh generator with built-in pre- and post-processing facilities. *International Journal for Numerical Methods in Engineering*, **79**, 1309–1331, <https://doi.org/10.1002/nme.2579>

- Gillespie, M.R., Crane, E.J. & Barron, H.F. 2013. *Study into the Potential for Deep Geothermal Energy in Scotland*. Volume 2 of 2. Scottish Government Project, <https://www2.gov.scot/resource/0043/00437996.pdf>
- GVL 2018. *Relative land motion map of the UK 2015–2017*, <https://www.geomaticventures.com/uk-map>
- Hall, A., Scott, J.A. & Shang, H. 2011. Geothermal energy recovery from underground mines. *Renewable and Sustainable Energy Reviews*, **15**, 916–924, <https://doi.org/10.1016/j.rser.2010.11.007>
- Hamm, V. & Bazargan Sabet, B. 2010. Modelling of fluid flow and heat transfer to assess the geothermal potential of a flooded coal mine in Lorraine, France. *Geothermics*, **39**, 177–186, <https://doi.org/10.1016/j.geothermics.2010.03.004>
- Hammeijer, J., Schlicke, A. *et al.* 2012. Fortissat minewater geothermal district heating project: case study. *Engineering & Technology Reference*, **1**, 1–8, <https://doi.org/10.1049/etr.2016.0087>
- Helm, P.R., Davie, C.T. & Glendinning, S. 2013. Numerical modelling of shallow abandoned mine working subsidence affecting transport infrastructure. *Engineering Geology*, **154**, 6–19, <https://doi.org/10.1016/j.enggeo.2012.12.003>
- Holloway, S., Jones, N., Creedy, D. & Garner, K. 2002. *Can new technologies be used to exploit the coal in the Yorkshire–Nottinghamshire coalfield?* Yorkshire Geological Society.
- House of Commons Energy and Climate Committee 2016. *2020 Renewable Heat and Transport Targets*. House of Commons, <https://publications.parliament.uk/pa/cm201617/cmselect/cnenergy/173/17302.htm>
- Jaiswal, A. & Shrivastva, B.K. 2009. Numerical simulation of coal pillar strength. *International Journal of Rock Mechanics and Mining Sciences*, **46**, 779–788, <https://doi.org/10.1016/j.ijrmms.2008.11.003>
- Jardon, S., Ordóñez, A., Álvarez, R., Cienfuegos, P. & Loredó, J. 2013. Mine water for energy and water supply in the central coal basin of Asturias (Spain). *Mine Water and the Environment*, **32**, 139–151, <https://doi.org/10.1007/s10230-013-0224-x>
- Jessop, A. 1995. Geothermal energy from old mines at Springhill, Nova Scotia, Canada. *Proceedings*, **17**, 463–468.
- Kolditz, O., Bauer, S. *et al.* 2012. OpenGeoSys: An open-source initiative for numerical simulation of thermo-hydro-mechanical/chemical (THM/C) processes in porous media. *Environmental Earth Sciences*, **67**, 589–599, <https://doi.org/10.1007/s12665-012-1546-x>
- Kruse, N.A. & Younger, P.L. 2009. Development of thermodynamically-based models for simulation of hydrogeochemical processes coupled to channel flow processes in abandoned underground mines. *Applied Geochemistry*, **24**, 1301–1311, <https://doi.org/10.1016/j.apgeochem.2009.04.003>
- Loredó, C., Roqueñi, N. & Ordóñez, A. 2016. Modelling flow and heat transfer in flooded mines for geothermal energy use: A review. *International Journal of Coal Geology*, **164**, 115–122, <https://doi.org/10.1016/j.coal.2016.04.013>
- Loredó, C., Ordóñez, A. *et al.* 2017. Hydrochemical characterization of a mine water geothermal energy resource in NW Spain. *Science of the Total Environment*, **576**, 59–69, <https://doi.org/10.1016/j.scitotenv.2016.10.084>
- Ma, X. & Zoback, M.D. 2017. Laboratory experiments simulating poroelastic stress changes associated with depletion and injection in low-porosity sedimentary rocks. *Journal of Geophysical Research: Solid Earth*, **122**, 2478–2503, <https://doi.org/10.1002/2016JB013668>
- Malolepszy, Z. 2003. Low temperature, man-made geothermal reservoirs in abandoned workings of underground mines. *Proceedings Twenty-Eighth Workshop on Geothermal Reservoir Engineering*, 27–29 January, Stanford University, Stanford, CA.
- McDermott, C., Williams, J. *et al.* 2016. Screening the geomechanical stability (thermal and mechanical) of shared multi-user CO<sub>2</sub> storage assets: A simple effective tool applied to the Captain Sandstone Aquifer. *International Journal of Greenhouse Gas Control*, **45**, 43–61, <https://doi.org/10.1016/j.ijggc.2015.11.025>
- Monaghan, A.A., Starcher, V., Dochartaigh, B.É.Ó., Shorter, K. & Burkin, J. 2018. *UK Geoenergy Observatories: Glasgow Geothermal Energy Research Field Site – Science Infrastructure*, <https://ukgeos.ac.uk/observatories/glasgow>
- Murali Mohan, G., Sheorey, P.R. & Kushwaha, A. 2001. Numerical estimation of pillar strength in coal mines. *International Journal of Rock Mechanics and Mining Sciences*, **38**, 1185–1192, [https://doi.org/10.1016/S1365-1609\(01\)00071-5](https://doi.org/10.1016/S1365-1609(01)00071-5)
- NCB 1972. *Design of Mine Layouts: With Reference to Geological and Geometrical Factors*. Working Party Report. National Coal Board, GB.
- NCB 1975. *Subsidence Engineers' Handbook*. National Coal Board, GB.
- Ordóñez, A., Jardon, S., Álvarez, R., Andrés, C. & Pendás, F. 2012. Hydrogeological definition and applicability of abandoned coal mines as water reservoirs. *Journal of Environmental Monitoring*, **14**, 2127, <https://doi.org/10.1039/c2em11036a>
- Preisig, G., Eberhardt, E., Smithyman, M., Preh, A. & Bonzanigo, L. 2016. Hydromechanical rock mass fatigue in deep-seated landslides accompanying seasonal variations in pore pressures. *Rock Mechanics and Rock Engineering*, **49**, 2333–2351, <https://doi.org/10.1007/s00603-016-0912-5>
- Renz, A., Rühaak, W., Schätzl, P. & Diersch, H.J.G. 2009. Numerical modeling of geothermal use of mine water: Challenges and examples. *Mine Water and the Environment*, **28**, 2–14, <https://doi.org/10.1007/s10230-008-0063-3>
- Rodríguez, R. & Díaz, M.B. 2009. Analysis of the utilization of mine galleries as geothermal heat exchangers by means a semi-empirical prediction method. *Renewable Energy*, **34**, 1716–1725, <https://doi.org/10.1016/j.renene.2008.12.036>
- Salmi, E.F., Nazem, M. & Karakus, M. 2017. The effect of rock mass gradual deterioration on the mechanism of post-mining subsidence over shallow abandoned coal mines. *International Journal of Rock Mechanics and Mining Sciences*, **91**, 59–71, <https://doi.org/10.1016/j.ijrmms.2016.11.012>
- Sizer, K.E. & Gill, M. 2000. Pillar failure in shallow coal mines — a recent case history. *Mining Technology. Transactions of the Institution of Mining and Metallurgy: Section A*, **109**, <https://doi.org/10.1179/mmt.2000.109.3.146>
- Sowter, A., Athab, A., Novellino, A., Grebby, S. & Gee, D. 2017. Supporting energy regulation by monitoring land motion on a regional and national scale: A case study of Scotland. *Proceedings of the Institution of Mechanical Engineers, Part A: Journal of Power and Energy*, **232**, 095765091773722, <https://doi.org/10.1177/0957650917737225>
- The Scottish Government 2018. *Energy in Scotland 2018*, <https://www2.gov.scot/Topics/Statistics/Browse/Business/Energy/EIS/EIS2018data>
- URS 2014. *Bilston Glen Scoping Study 47068917*. Prepared for The Coal Authority.
- Verhoeven, R., Willems, E., Harcouët-Menou, V., De Boever, E., Hiddes, L., Veld, P.O.t. & Demollin-Schneiders, E. 2014. Minewater 2.0 project in Heerlen the Netherlands: Transformation of a geothermal mine water pilot project into a full scale hybrid sustainable energy infrastructure for heating and cooling. *Energy Procedia*, **46**, 58–67, <https://doi.org/10.1016/j.egypro.2014.01.158>
- Wang, W., Kosakowski, G. & Kolditz, O. 2009. A parallel finite element scheme for thermo-hydro-mechanical (THM) coupled problems in porous media. *Computers & Geoscience*, **35**, 1631–1641, <https://doi.org/10.1016/j.cageo.2008.07.007>
- Wolkersdorfer, C. 2008. *Water Management at Abandoned Flooded Underground Mines: Fundamentals, Tracer Tests, Modelling, Water Treatment*. Springer, Berlin, <https://doi.org/10.1007/978-3-540-77331-3>
- Younger, P.L. 2001. Mine water pollution in Scotland: Nature, extent and preventative strategies. *Science of the Total Environment*, **265**, 309–326, [https://doi.org/10.1016/S0048-9697\(00\)00673-2](https://doi.org/10.1016/S0048-9697(00)00673-2)
- Younger, P.L. & Adams, R. 1999. *Predicting Mine Water Rebound*. R&D Technical Report W179. Environment Agency, Bristol.
- Younger, P.L. & Robins, N.S. 2002. Challenges in the characterization and prediction of the hydrogeology and geochemistry of mined ground. In: Younger, P.L. & Robins, N.S. (eds) *Mine Water Hydrogeology and Geochemistry*. Geological Society, London, Special Publications, **198**, 1–16, <https://doi.org/10.1144/GSL.SP.2002.198.01.01>